NRC Publications Archive
Archives des publications du CNRC

Geometrical modeling of laser ablation
Vatsya, S.R.; Bordatchev, E.V.; Nikumb, S.K.

This publication could be one of several versions: author's original, accepted manuscript or the publisher's version. / La version de cette publication peut être l'une des suivantes : la version prépublication de l'auteur, la version acceptée du manuscrit ou la version de l'éditeur.

Publisher's version / Version de l'éditeur:

ICALEO Conference Proceedings, 2002

NRC Publications Record / Notice d'Archives des publications de CNRC:
https://nrc-publications.canada.ca/eng/view/object/?id=0eb4e847-d7a7-4e83-907c-7d799b072c9b
https://publications-cnrc.canada.ca/fra/voir/objet/?id=0eb4e847-d7a7-4e83-907c-7d799b072c9b

Questions? Contact the NRC Publications Archive team at
PublicationsArchive-ArchivesPublications@nrc-cnrc.gc.ca. If you wish to email the authors directly, please see the first page of the publication for their contact information.

Vous avez des questions? Nous pouvons vous aider. Pour communiquer directement avec un auteur, consultez la première page de la revue dans laquelle son article a été publié afin de trouver ses coordonnées. Si vous n'arrivez pas à les repérer, communiquez avec nous à PublicationsArchive-ArchivesPublications@nrc-cnrc.gc.ca.

National Research Council Canada   Conseil national de recherches Canada

Canada

Geometrical modeling of laser ablation

by

S.R. Vatsya, E.V. Bordatchev and S.K. Nikumb

Integrated Manufacturing Technologies Institute
National Research Council of Canada
800 Collip Circle, London, ON, Canada, N6G 4X8

Abstract

Recent advances in the laser machining technology have made it possible to fabricate parts and features with high accuracy and precision, using high-powered, short-pulsed, Q-switched lasers. To determine the machining parameters to obtain desired geometrical quality, an understanding of the relationship between the process parameters and the resulting surface profile, is necessary. In the present study, we adopt a geometrical approach, which coupled with the material properties and machining process parameters, yields a model for the surface profile of the region ablated by a laser pulse. Energy incident upon an infinitesimal area of the surface is transferred in the outward normal direction, and the depth of the ablation depends on the laser-material interaction and the process parameters. This determines the modified surface profile an infinitesimal time later, yielding a nonlinear partial differential equation, which is then integrated to determine the profile after a given time period. Theoretical predictions and the experimental results are compared and discussed.

1. Introduction

Availability of high powered, short pulsed, lasers, and the technological advances in the related areas have made it possible to machine features with high accuracy and precision,[1,2] stimulating interest in the underlying processes. The phenomena of significance depend on the material properties, e.g., the response of metals to laser irradiation is largely determined by its thermal diffusion properties, the ablation of dielectrics is governed mainly by the generation of new electrons in the conduction band by impact ionization,[3,4] and the semiconductors behave somewhere in between. In addition, the pulse width determines the magnitude of the electron-lattice coupling impacting upon the quality of the ablated surface[5]. In the present paper, we restrict to ablation of metals by the nanopulse lasers.

Most of the modeling work for the metals, so far has focused on determining the depths and diameters of the ablated region.[5,6] Incident optical energy is diffused as heat into the metal, raising the temperature of the surface to the melting point. The heat transfer prior to the threshold, when the phase change occurs, is quite adequately described by a one dimensional diffusion equation.[6,7] Incident energy, in excess of the threshold fluence, then melts and evaporates the material. Energy still continues to be lost into the lattice as the melting temperature is maintained at the surface. The depth estimates are then obtained from an Arrhenius type equation.[8,9]

In the present article, we describe the evolution of the surface profile with time, in more detail, combining the material properties, which determine the energy used for ablation, with the geometrical properties of the surface at a particular time, which

determine the direction of absorption of the energy to create the profile at an infinitesimal time later. The heat diffusion equation is used to determine the time at which the melting, and the ablation process, begins. During the material removal phase, the properties of the ablated surface at a given time t are used to determine the surface profile at a later time $(t + dt)$, as follows. At time t, the incident laser radiation reflects from the tangent plane to the ablated surface at each point on the surface, transferring energy into the lattice in the direction of the normal to the tangent surface at that point. This energy melts and evaporates the material, centered about the outward normal to the tangent plane at each point, which determines the evolution of the surface after an infinitesimal increment dt in time, yielding a nonlinear differential equation, which is then integrated to obtain the profile of the ablated surface at an arbitrary time. The energy needed to maintain the equilibrium temperature should be subtracted from the incident energy to determine the energy available to evaporate the material. Material removal terminates when the laser energy is insufficient to melt the solid and sustain the diffusion.

A comparison of the experimentally observed surface profile is made with the theoretical predictions for machining of copper and brass foils by lasers of pulse widths in the nanosecond range, starting with a flat surface. In view of this, and the radial symmetry of the laser beam, the equations reduce to a radially symmetric system, simplifying the calculations. Energy distribution in the laser beam was assumed to be Gaussian, both with respect to space and time. The diffusion during the ablation phase was found to be small, and therefore, was neglected. Also, the ablation process was found to continue until the laser power reduced to a small fraction of the peak power. Therefore, the material removal termination time was assumed to be infinite. The model is found to describe the observed surface profile adequately.

2. Geometrical formulation of the ablated surface

The geometrical description of the evolution of the ablated surface with time, developed here, is material independent. The material properties impact upon the energy available and needed for ablation. During the initial phase, the absorbed heat is used to raise the temperature of the material to the melting point, when the ablation process begins, at time t equal to t_{melt}. In this section, we confine to the evolution of the surface during the ablation phase, $t_{melt} \leq t \leq t_{max}$, where t_{max} is the time when the laser energy is no longer sufficient to maintain the temperature of the surface at the melting point. The onset and termination of the ablation process and the energy available during the material removal phase are determined in Sec. 3.

Starting with an arbitrary point $P(t) = (x, y, z(x, y, t))$, at time t, on the ablated surface, $S(t)$, the purpose is to determine the corresponding point at an infinitesimal time later. Since the initial surface, is known, this is sufficient to determine the surface at all later times.

The tangent space $\mathsf{T}_P(t)$ to $S(t)$ at $P(t)$ is spanned by the basis vectors e_x and e_y, given by

$$e_x = (1, 0, \frac{\partial z}{\partial x}), \text{ and } e_y = (0, 1, \frac{\partial z}{\partial y}).$$

A laser beam incident and reflected at $P(t)$ transfers momentum, and energy, in the direction of the outward normal $v(x,y,t)$ to the surface $T_P(t)$ at $P(t)$, given by

$$v(x,y,z(t)) = \frac{(e_y \times e_x)}{|(e_y \times e_x)|} = \frac{1}{\eta(x,y,z(t))}\left(\frac{\partial z}{\partial x}, \frac{\partial z}{\partial y}, -1\right) \tag{1}$$

where $(e_y \times e_x)$ is the vector product of the vectors e_y and e_x, and

$$\eta(x,y,z(t)) = \sqrt{\left[1 + \left(\frac{\partial z}{\partial x}\right)^2 + \left(\frac{\partial z}{\partial y}\right)^2\right]},$$

is the area enclosed by the vectors e_x and e_y, which projects on the surface element of unit area in the $X - Y$ plane.

Let $I(x,y,t)$ and a_θ be the laser power and the absorption coefficient, where θ is the angle between the reflected beam and the inward normal. The case $\theta = 0$ corresponds to a vertical laser beam incident upon the $X - Y$ plane. The intensity at $P(t)$ from time t to $(t+dt)$ is equal to $[I(x,y,t)\ dt]/\eta(x,y,z(t))$, and thus, the absorbed energy per unit area I_{abs} is given by, $I_{abs} = [a_\theta I(x,y,t)\ dt]/\eta(x,y,z(t))$. The absorption coefficient also depends on $\theta(x,y,z(t))$, which is assumed to be directly proportional to the transferred momentum, i.e.,

$$a_\theta(x,y,z(t)) = a_0 \cos(\theta) = a_0(-\hat{z} \bullet v[x,y,z(t)]) = [a_0/\eta(x,y,z(t))],$$

where $\hat{z}$ is the unit vector in the upward vertical direction. Consequently,

$$I_{abs} = [a_0 I(x,y,t)\ dt]/\eta^2(x,y,z(t)).$$

Let $(\Delta J\ dt)$ be the corresponding energy per unit area, diffused into the lattice during the material removal phase. The distance $\sigma(x,y,z(t))\ dt$, in the direction of the outward normal, of the ablated volume during the time dt is given by,

$$\sigma(x,y,z(t))\ dt = \{[a_0 I(x,y,t)/\eta^2(x,y,z(t) - \Delta J\ ]/E_H\}dt \tag{2}$$

where E_H is the heat required to melt and evaporate the unit volume of the material.

3

From Eqs. (1) and (2), the point $P(t+dt) = [P(t) + dP(t)]$, on the surface at time $(t+dt)$, corresponding to $P(t)$, is given by,

$$dP(t) = (dx, \ dy, \ dz(x,y,t)) = \alpha(x,y,z(t)) \left(\frac{\partial z}{\partial x}, \ \frac{\partial z}{\partial y}, \ -1 \right) dt \tag{3}$$

where

$$\alpha(x,y,z(t)) \ dt = [\sigma(x,y,z(t)) \ dt]/\eta(x,y,z(t)),$$

and hence,

$$\frac{dx}{dt} = \alpha(x,y,z(t)) \frac{\partial z}{\partial x}, \qquad \frac{dy}{dt} = \alpha(x,y,z(t)) \frac{\partial z}{\partial y},$$

and

$$\frac{dz}{dt} = \left[\frac{\partial z}{\partial t} + \frac{dx}{dt} \frac{\partial z}{\partial x} + \frac{dy}{dt} \frac{\partial z}{\partial y} \right] = - \alpha(x,y,z(t)),$$

i.e.,

$$\frac{\partial z}{\partial t} = - \alpha(x,y,z(t)) \left[\left(\frac{\partial z}{\partial x} \right)^2 + \left(\frac{\partial z}{\partial y} \right)^2 + 1 \right] \tag{4}$$

Appropriate substitutions, from Eqs. (1), (2) and (3), into Eq. (4), yield the following equation for the time evolution of the ablated surface:

$$\frac{\partial z}{\partial t} + \frac{a_0 \ I(x,y,t)}{E_H} \left[1 + \left(\frac{\partial z}{\partial x} \right)^2 + \left(\frac{\partial z}{\partial y} \right)^2 \right]^{-\frac{1}{2}} - \frac{\Delta J}{E_H} \left[1 + \left(\frac{\partial z}{\partial x} \right)^2 + \left(\frac{\partial z}{\partial y} \right)^2 \right]^{\frac{1}{2}} = 0 \tag{5}$$

The surface profile is obtained by solving Eq. (5), for t from t_{melt} to t_{max} with $z(x,y,t_{melt})$ being the initial, known, profile. Procedures to determine t_{melt}, and ΔJ are described in the following section. The termination point t_{max} is determined by ΔJ.

3. Thermal diffusion

To determine the surface profile from Eq. (5) one needs the values of t_{melt}, ΔJ and t_{max}. Procedures to determine these quantities are described below using the thermal diffusion properties of the material.

4

The evolution of the temperature for $t < t_{melt}$, in response to the laser irradiation, is governed to a good degree of approximation by the one dimensional thermal diffusion equation,[8,10,11] which in the nanosecond regime reads[5,6,7] as,

$$\frac{\partial T_<}{\partial t} - \frac{\partial}{\partial \xi} D \frac{\partial T_<}{\partial \xi} = \frac{I(x,y,t) a_0 \alpha}{C} \exp(-\alpha \xi)$$

$$T_<(\xi, -\infty) = 0, \quad T_<(\infty, t) = 0, \quad \frac{\partial T_<(\xi,t)}{\partial \xi} = 0 \quad at \quad \xi = 0,$$

(6)

where $T_<(\xi,t)$ is the electron temperature at location ξ along the normal to the appropriate surface, which during this phase is the initial surface. For a flat surface, ξ is the coordinate representing the vertical direction with the origin at the surface. In Eq. (6), D, C and α are the diffusitivity, electron specific heat, and the inverse of the optical depth of the material, respectively, and the laser power, is given by,

$$I(x,y,t) = I_0 \exp[-2(x^2 + y^2)/(D_B/2)^2 - \kappa(t/\tau_P)^2]$$

(7)

where $\kappa = 4\log(2)$, τ_P is the pulse width, I_0 is the peak power reached at the center of the beam at zero time, and D_B is the beam diameter.

In the present long pulse regime the electron and the lattice temperatures are almost equal, reducing the general diffusion equation[8,10,11] to Eq. (6). Also, the diffusion function D, although not constant at high temperatures, it is assumed to be constant for the present. This approximation is quite adequate within the degree of the accuracy of the experimental data available.[8,12]

With these simplifying assumptions, the solution of Eq. (6) is given by,

$$T_<(\xi,t) = \frac{a_0 \alpha}{C} \int_0^\infty dk \ \cos(k\xi) \ \frac{\alpha}{(\alpha^2 + k^2)} \int_{-\infty}^t dt' \ \exp[-Dk^2(t-t')] \ I(t')$$

$$= \frac{a_0 \alpha}{C} \int_0^\infty dk \ \cos(k\xi) \ \frac{\alpha}{(\alpha^2 + k^2)} \int_0^\infty d\tau \ \exp[-Dk^2\tau] \ I(t-\tau)$$

(8)

The expression given by Eq. (8) implies that $T_<(\xi,\infty) = 0$, in addition to the given condition, $T_<(\xi,-\infty) = 0$, which in turn can be used to express the Fourier transform $\hat{T}_<(\xi,\omega)$ of $T_<(\xi,t)$ as,

$$\hat{T}_<(\xi,\omega) = \frac{I_0 a_0 \exp[-\omega^2/(4\kappa)]}{C\sqrt{2\kappa} \ (D\alpha^2 + i\omega)} \left[\alpha(i+1)\sqrt{\frac{D}{2\omega}} \ \exp[(i-1)\sqrt{\frac{\omega}{2D}} \ \xi] - \exp(-\alpha\xi) \right]$$

(9)

The temperature $T_<(\xi,t)$ is determined by $\hat{T}_<(\xi,\omega)$, as its inverse Fourier transform, which determines t_{melt} from $T_<(0,t_{melt}) = T_{melt}$.

For $t > t_{melt}$, the laser energy is used in melting and evaporating the material with the temperature at the surface of the ablated region maintained at T_{melt}. Since the laser energy is absorbed by the material above the bottom of the melt, there is no source of heat below it. Hence the heat diffusion in the material below the melt is governed by,

$$\frac{\partial T_>}{\partial t} - \frac{\partial}{\partial \zeta} D \frac{\partial T_>}{\partial \varsigma} = 0, \quad t \geq t_{melt}, \quad \varsigma \geq 0,$$

$$T_>(0,t) = T_{melt}, \quad \frac{\partial T_>(\varsigma,t)}{\partial \varsigma} \xrightarrow[\varsigma \to \infty]{} 0.$$

(10)

In Eq. (10), ς is the coordinate along the outward normal to the ablated surface with the origin at the bottom of the melt, which defines a variable boundary. However, the effects of the variable boundary, detailed description of the thermal transfer inside the liquid metal, and similar effects at the vaporization phase, will be neglected for the present.

To uniquely define the solution of Eq. (10), one boundary condition with respect to time is also needed, which is determined as follows. Let $\xi(\varsigma)$ be the value of ξ for a given ς, both coordinates placed along the same axis. We assume that $T_<(\xi(0), t_{melt}) = T_<(0, t_{melt}) = T_{melt}$, which is a mild assumption in view of the fact that the temperature gradient at $\xi = 0$ for $t \leq t_{melt}$ is equal to zero. This assumption is also consistent with neglecting the effects of the variable boundary. Essential equivalence of ξ and ς implied in this assumption, also requires rotation symmetry of $T_<(\xi,t)$ in the neighborhood of the ablated region, which is justified by the validity of the one dimensional diffusion model. With these assumptions, the additional condition is given by,

$$T_>(\varsigma,t_{melt}) = T_<(\xi(\varsigma),t_{melt}) \tag{11}$$

The solution of Eq. (10) is now given by

$$T_>(\varsigma,t) = T_<(\xi(\varsigma),t_{melt}) + \frac{2}{\pi} \int_0^\infty \frac{dk}{k^2} \sin(k\varsigma)\left(1 - \exp[Dk^2(t_{melt} - t)]\right) \ddot{T}_<^{sf}(k), \tag{12}$$

where

$$\ddot{T}_<^{sf}(k) = \int_0^\infty d\varsigma \; \sin(k\varsigma) \frac{\partial^2 T_<(\xi(\varsigma),t_{melt})}{\partial \varsigma^2}$$

The heat flux ΔJ is determined by $T_>(\varsigma,t)$:

$$\Delta J(\varsigma,t) = -CD \frac{\partial T_>(\varsigma,t)}{\partial \varsigma} \tag{13}$$

The ablation process ceases when the heat flux at the surface exceeds the supplied heat. Thus, t_{max} is determined by,

$$a_0 I(x, y, t_{max}) = \eta^2(x, y, z(t_{max})) \ \Delta J(0, t_{max}) \tag{14}$$

4. Results and discussion

Present model was tested by comparing the theoretical predictions with the experimental observations of the laser-ablated surfaces in brass and copper foils. Thin foils of copper and brass with of thickness of 70 μm were mounted on a specially built vacuum fixture, which was equipped with features to remove any surface distortions, striations and unevenness while loading. All the experiments with copper foils were carried out using an electro-optically Q-switched diode pumped solid state laser HPO-1000 (by Continuum Inc.) which has pulse width of 9.8 ns, wavelength of 532 nm and a shot-to-shot stability of 95.0% for TEM00 mode and an appropriate beam delivery system. The AMOCO OEM 1064-1000Q laser by AMOCO Laser Company was used to machine the brass foils. This laser has a pulsewidth of 16.2 ns at a pulse repetition rate of 1.0 kHz with a wavelength of 1064 nm and a pulse to pulse instability of less than 6.5% for linear polarization and TEM00 mode. Different lasers were used to determine the effects of the laser properties on the surface profile. The positioning accuracy of the motion system was of the order of 0.5 μm in the X and Y axes. The pulse energy measurements were carried out using a calibrated laser power meter (model: TMP-300 from Gentec Inc). A single pulse from the laser creates bowl-like craters on the foil. The distance between craters was set to greater than 30 μm to avoid overlapping of the heat-affected zones. An optical microscope and a WYKO surface profilometer were used to measure the crater geometry and the surface topology on the machined foils. An example of the typical laser machined craters and the corresponding profiles of the ablated surface for a brass foil are shown in Figure 1.
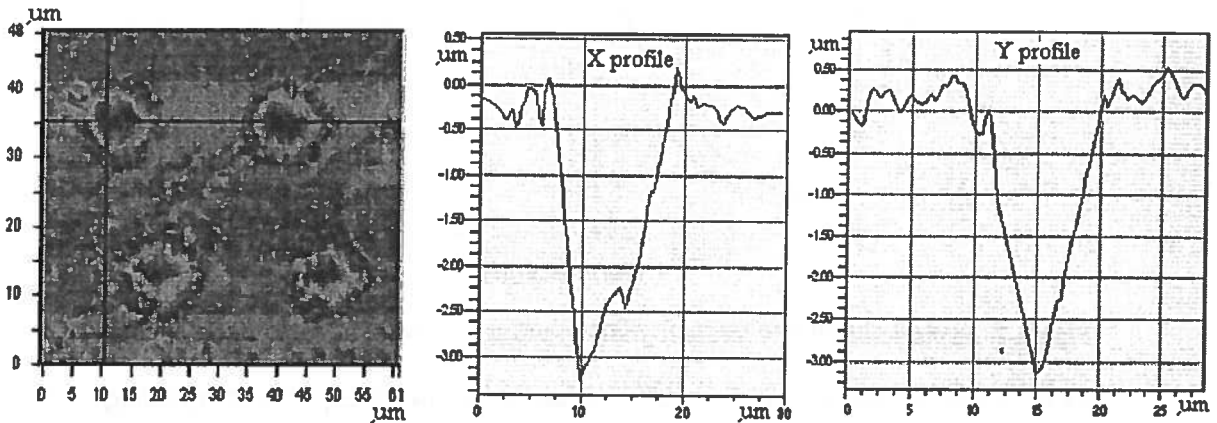

Figure 1. Typical laser machined craters and the corresponding profiles of the ablated surface (brass foil).

For the present, radially symmetric approximation, the profile depths along X and Y axes were averaged to obtain the profile with respect to the radial distances. Also, the

data for comparison was taken to be the average over a number of measurements, with the statistical deviations used to determine the surface profile within the experimental accuracy.

The laser power distribution was assumed to be Gaussian, both in space and time, given by Eq. (7), with I_0 determined by

$$
\begin{aligned}
E_{pulse} &= I_0 \int_{-\infty}^{\infty} dt \int_{-\infty}^{\infty} dx \int_{-\infty}^{\infty} dy \ \exp[-2(x^2 + y^2)/(D_B/2)^2 - \kappa(t/\tau_P)^2] \\
&= \frac{1}{8}\pi D_B^2 I_0 \tau_P \sqrt{\frac{\pi}{\kappa}}
\end{aligned}
\tag{15}
$$

where $\exp(\kappa) = 16$.

The temperature $T_<(\xi,t)$, determined by Eq. (9), was computed by using the standard Fast Fourier Transform routine. Time evolution of $T_<(\xi,t)$ for copper with $E_{pulse} = 225 \ \mu J$ is shown in Figure 2. The temperature on the surface rises quickly after the irradiation starts, at $t_{melt} = -1.03$ in units of the pulse-width, i.e., by the time the laser power has increased from zero to about 1/16 th of its peak power.
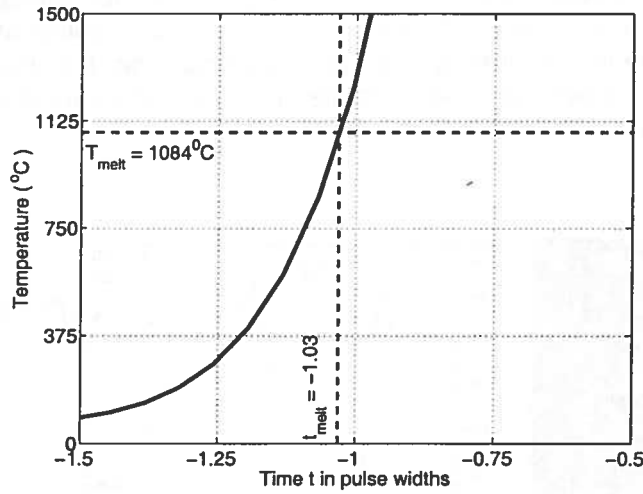

Figure 2. Approach of temperature to melting point, with time, at the surface of copper.

The profile of the ablated surface is obtained from Eq. (5), neglecting ΔJ, reducing it to

$$
\frac{\partial z}{\partial t} = -\frac{a_0 \ I(r,t)}{E_H}\left[1+\left(\frac{\partial z}{\partial r}\right)^2\right]^{-\frac{1}{2}}
\tag{16}
$$

8

The right side in Eq. (16) was evaluated by forward differencing with respect to the radial distance r, with origin at the center of the laser beam, and integrated by the forward Euler method starting at t_{melt}. Since the melting temperature is reached quite quickly after the irradiation begins, it was found that integrating Eq. (16) from $t = -\infty$, instead of t_{melt}, does not change the predicted profile significantly.
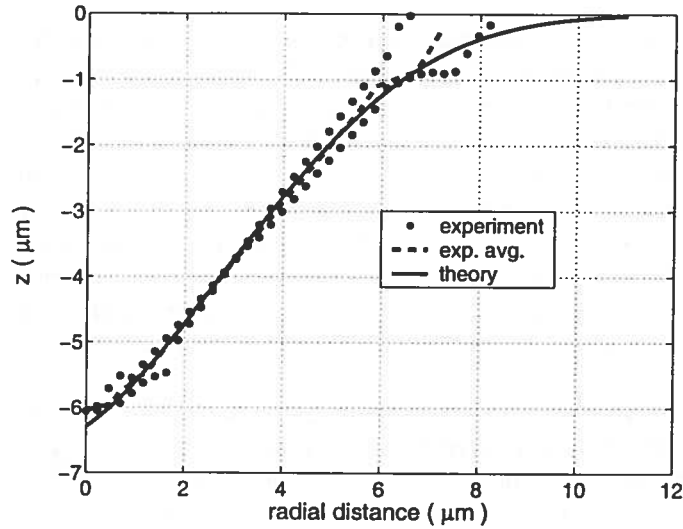

Figure 3. Comparison of theoretical and experimental copper surface profiles.

Theoretical predictions and the experimental observations are displayed in Figure 3 for copper, and in Figure 4 for brass. There are noticeable statistical variations in the experimental data. The observations selected are deemed to represent the observed profiles adequately.
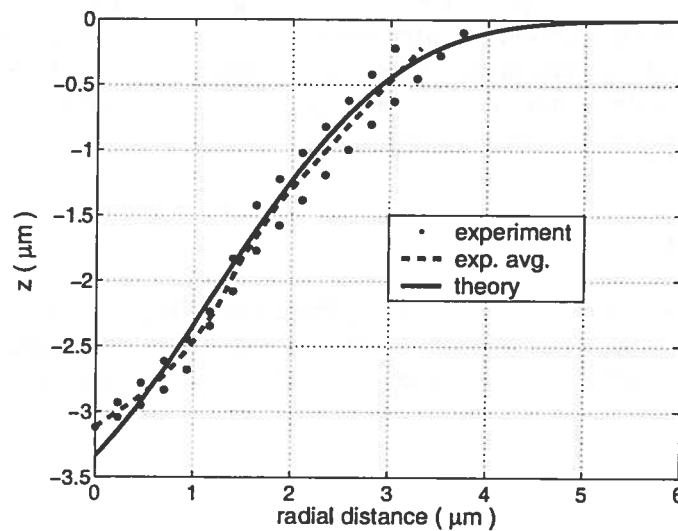

Figure 4. Comparison of theoretical and experimental brass surface profiles.

From Figs. 3 and 4, the agreement between the theoretical and the experimental values, for different lasers and materials, is quite satisfactory, indicating the adequacy of the geometrical approach to formulate the laser pulse ablated surfaces of metals.

5. Concluding remarks

We have developed a mathematical model to determine the detailed geometrical profile of the surface of the materials ablated by lasers, which has been lacking in the literature. Most of the work so far has been concentrated on estimating the depths and diameters of the bowl like craters formed during laser machining. The present approach combines the standard heat diffusion properties of the material with the geometrical properties of the surface to determine its evolution with respect to the time. The geometrical formulation is independent of the material and the laser specifics, which determine the amount of heat defused and the volume of the material ablated during a given time period. Thus the geometrical formulation presented here is applicable to study the surface profiles of essentially all materials irrespective of the laser used.

For comparison with the experimental observations, the foils of brass and copper were machined with lasers of pulse widths in the nanosecond range. The pulse width, together with the material properties, determines the diffusion equation that adequately describes the heat transfer into the material and the material properties determine the volume of the material melted and evaporated during a given time period. The geometrical considerations are used to determine the axis about which the ablated volume is located.

In the cases considered, the agreement between the theoretical predictions and the experimental observations is quite satisfactory, indicating the adequacy of the present formulation to describe the surface profile of the laser machined materials.

Present model can be improved further in several ways. The approximations used in the present study, although mild, should be investigated further. In particular, the initial surface often is not flat enough to justify the assumption of radial symmetry. Thus, an extension of the model to two dimensions is desirable. The formulation given here is quite complete in this and several other respects, but an implementation of these results will require additional numerical developments.

Acknowledgements

References

1. K. Venkatakrishnan, B. Tan and B.K.A. Ngoi, "Submicron holes in copper thin film ablated using femtosecond pulsed laser," Opt. Eng. **40**, 2892 (2001).
2. X. Liu, "Submicron lines in thin metallic films micromachined by an ultrafast laser oscillator," in Theoretical Digest, Conference on Lasers and Electro-Optics, 511 (1998).
3. S.R. Vatsya and S.K. Nikumb, "Modeling of laser-induced avalanche in dielectrics," J. Appl. Phys. 91, 344 (2001).
4. T. Apostolova and Y. Hahn, "Modeling of laser-induced breakdown in dielectrics with subpicosecond pulses," J. Appl. Phys. **88**, 1024 (2000).
5. B.N. Chichkov, C. Momma, S. Nolte, F. von Alvensleben and A. Tunnermann, "Femtosecond, picosecond and nanosecond laser ablation of solids," Appl. Phys. **A 63**, 109 (1996).
6. R.F. Wood and G.E. Giles, "Macroscopic theory of pulsed-laser annealing. I. Thermal transport and melting," Phys. Rev. B **23**, 2923 (1981).
7. R.F. Wood and G.E. Jellison, Jr., "Melting model of pulsed laser processing," in Semiconductors and semimetals, Vol. 23, PP. 166-246 (Academic Press, Inc., New York, 1984).
8. S. Nolte, C. Momma, H. Jacobs, A. Tunnermann, B.N. Chichkov, B. Wellegehausen and H. Welling, "Ablation of metals by ultrashort laser pulses," J. Opt. Soc. Am. **B 14**, 2716 (1997).
9. S.I. Anisimov, M.I. Tribel'skii and Ya. G. Epel'bausm, "Instability of plane wave evaporation front in interaction of laser radiation with a medium," Sov. Phys. JETP **51**, 802 (1980).
10. S.I. Anisimov, B.L. Kapeliovich and T.L. Perel'man, "Electron emission from metal surfaces exposed to ultrashort laser pulses," Sov. Phys., JETP **39**, 375 (1974).
11. M.I. Kagaov, I.M. Lifshitz and L.V. Tanatarov, "Relaxation between electrons and the crystalline lattice," Sov. Phys., JETP **4**, 173 (1957).
12. P.B. Corkum, F. Brunel and N.K. Sherman, "Thermal response of metals to ultrashort-pulse laser excitation," Phys. Rev. Lett. **61**, 2886 (1988).